Supplement of The Cryosphere, 20, 609–628, 2026
https://doi.org/10.5194/tc-20-609-2026-supplement

The Cryosphere Open Access EGU

Supplement of

Advancing snow data assimilation with a dynamic observation uncertainty

Devon Dunmire et al.

Correspondence to: Devon Dunmire (devon.dunmire@kuleuven.be)

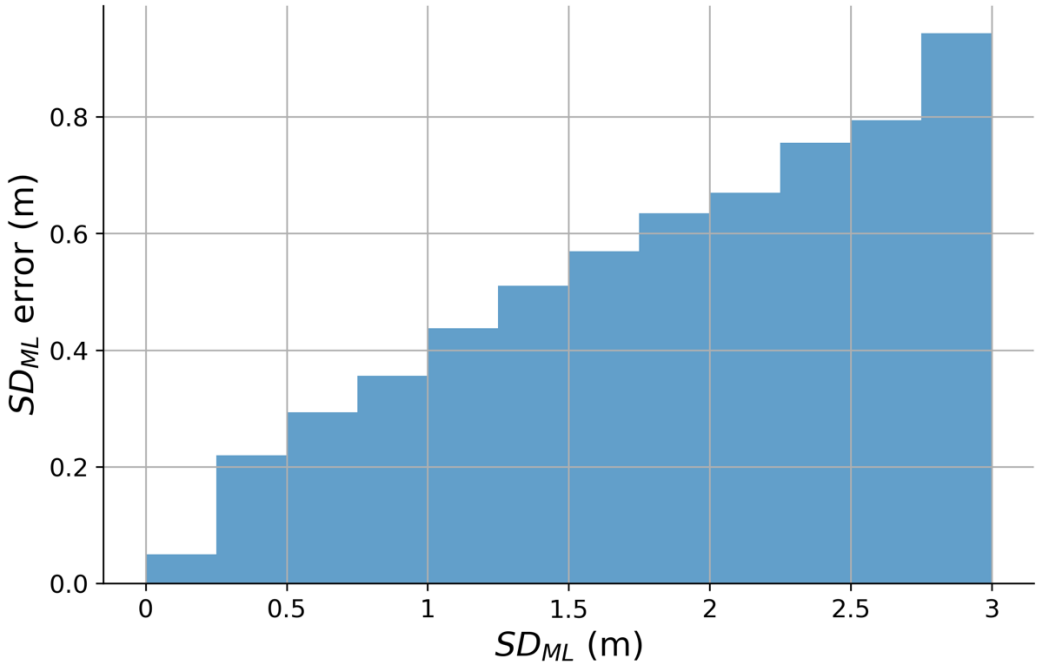

Figure S1 Actual observation error per bin of assimilated snow depth (SD_{ML}). The error is computed using 588 independent in-situ measurement sites.

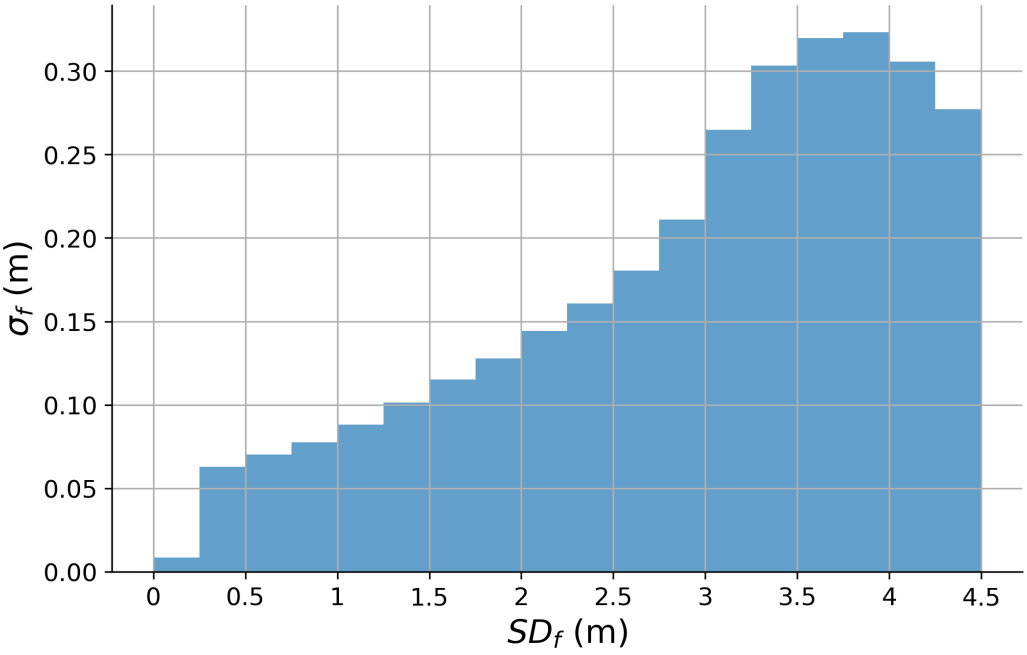

Figure S2 Standard deviation of the forecast error (σ_f) per bin of forecast snow depth (SD_f). σ_f is computed as the standard deviation of the OL ensembles.

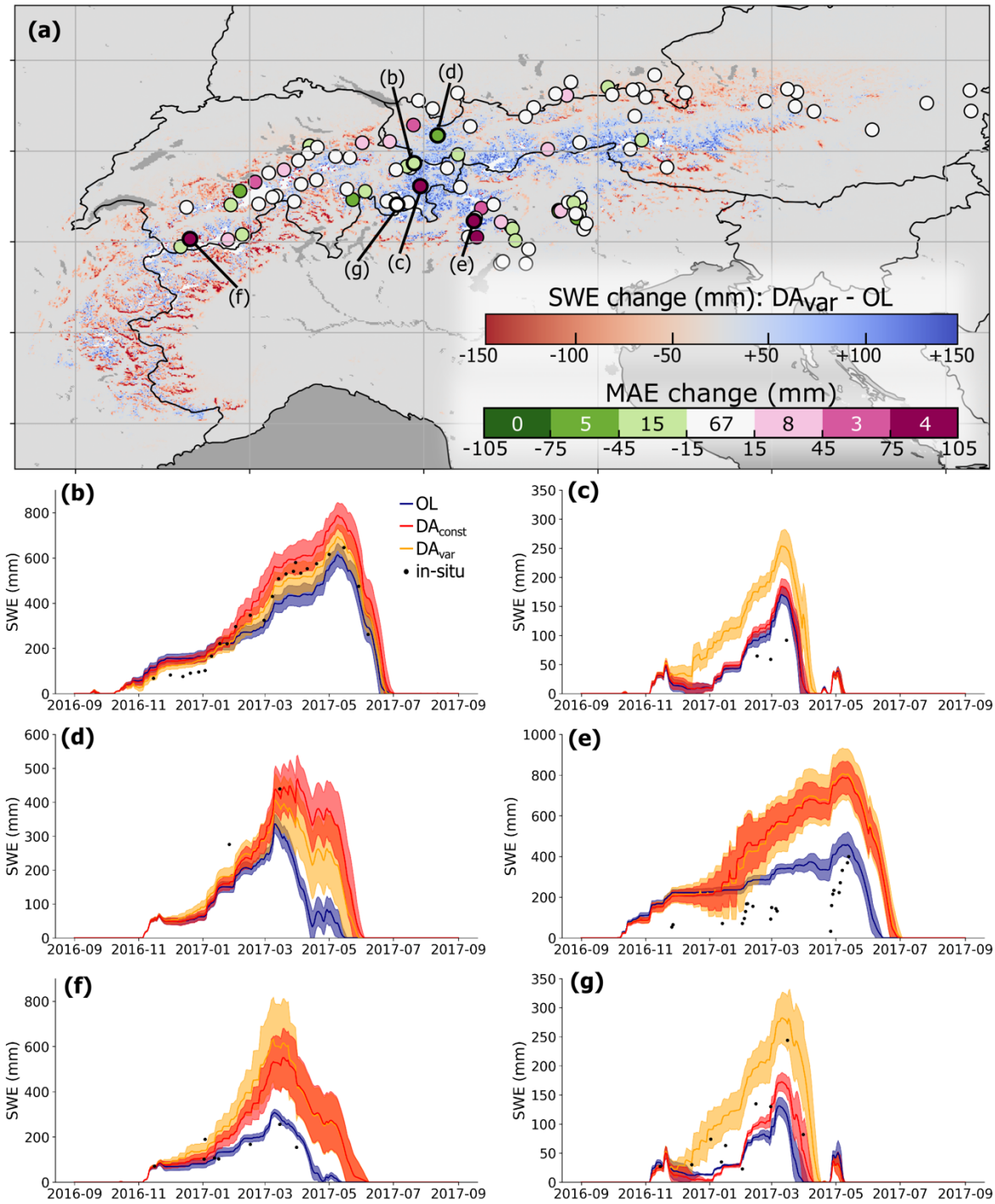

Figure S3 2017 SWE comparison. (a) Map of SWE changes (DA_{var} – OL), averaged during the period March 1 – 7, 2017. Sites with manual SWE measurements from the 2016/2017 snow season are plotted, colored according to the change in MAE between the DA_{var} and OL experiments. MAE changes are computed over the entire snow season. On the MAE change color bar, the number of sites that fall within each color range is indicated. (b-g) SWE timeseries from the three model experiments, compared with manual measurements (black dots) for in-situ measurement sites which are indicated in (a).

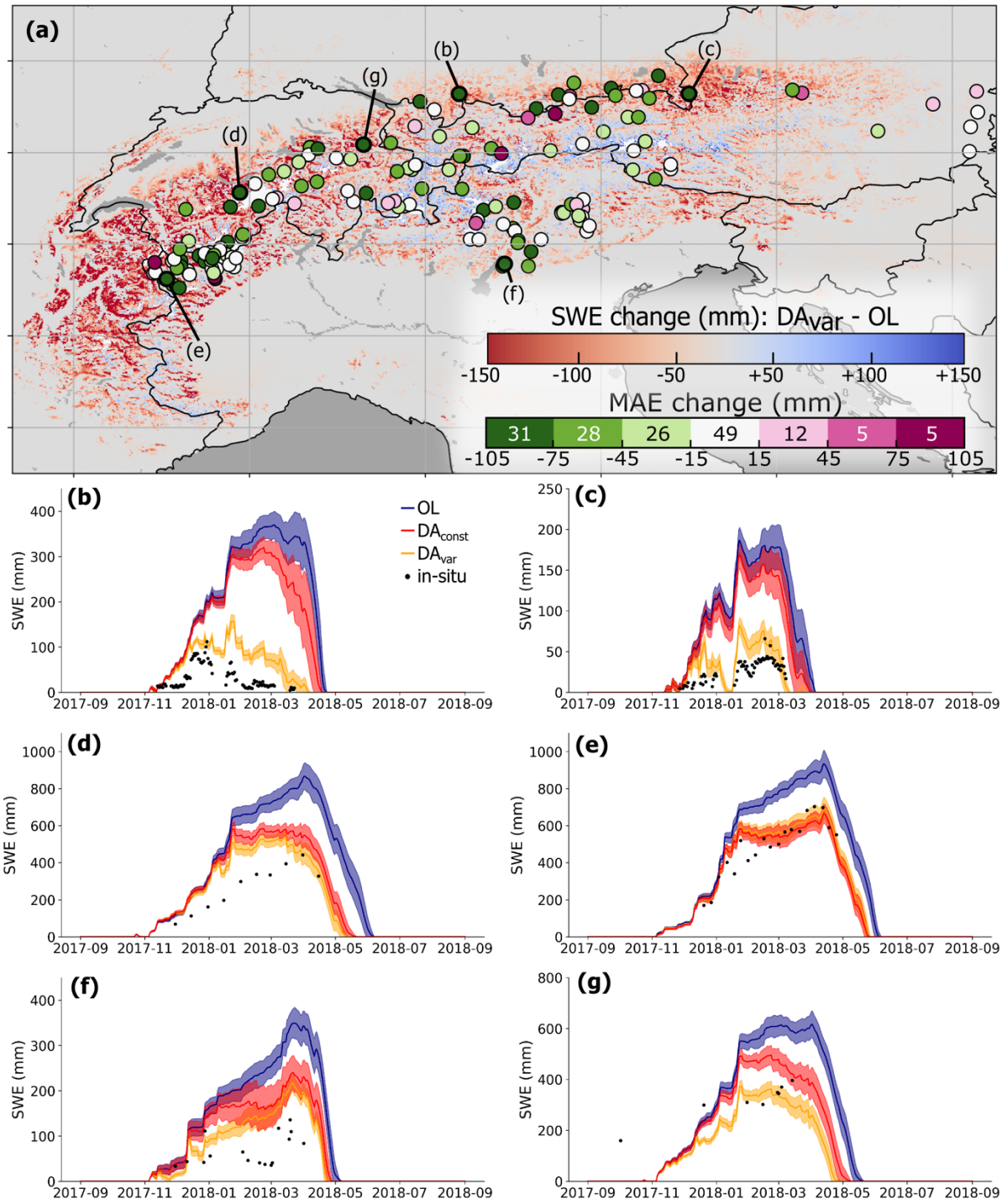

Figure S4 2018 SWE comparison. (a) Map of SWE changes (DA_{var} – OL), averaged during the period March 1 – 7, 2018. Sites with manual SWE measurements from the 2017/2018 snow season are plotted, colored according to the change in MAE between the DA_{var} and OL experiments. MAE changes are computed over the entire snow season. On the MAE change color bar, the number of sites that fall within each color range is indicated. (b-g) SWE timeseries from the three model experiments, compared with manual measurements (black dots) for in-situ measurement sites which are indicated in (a).

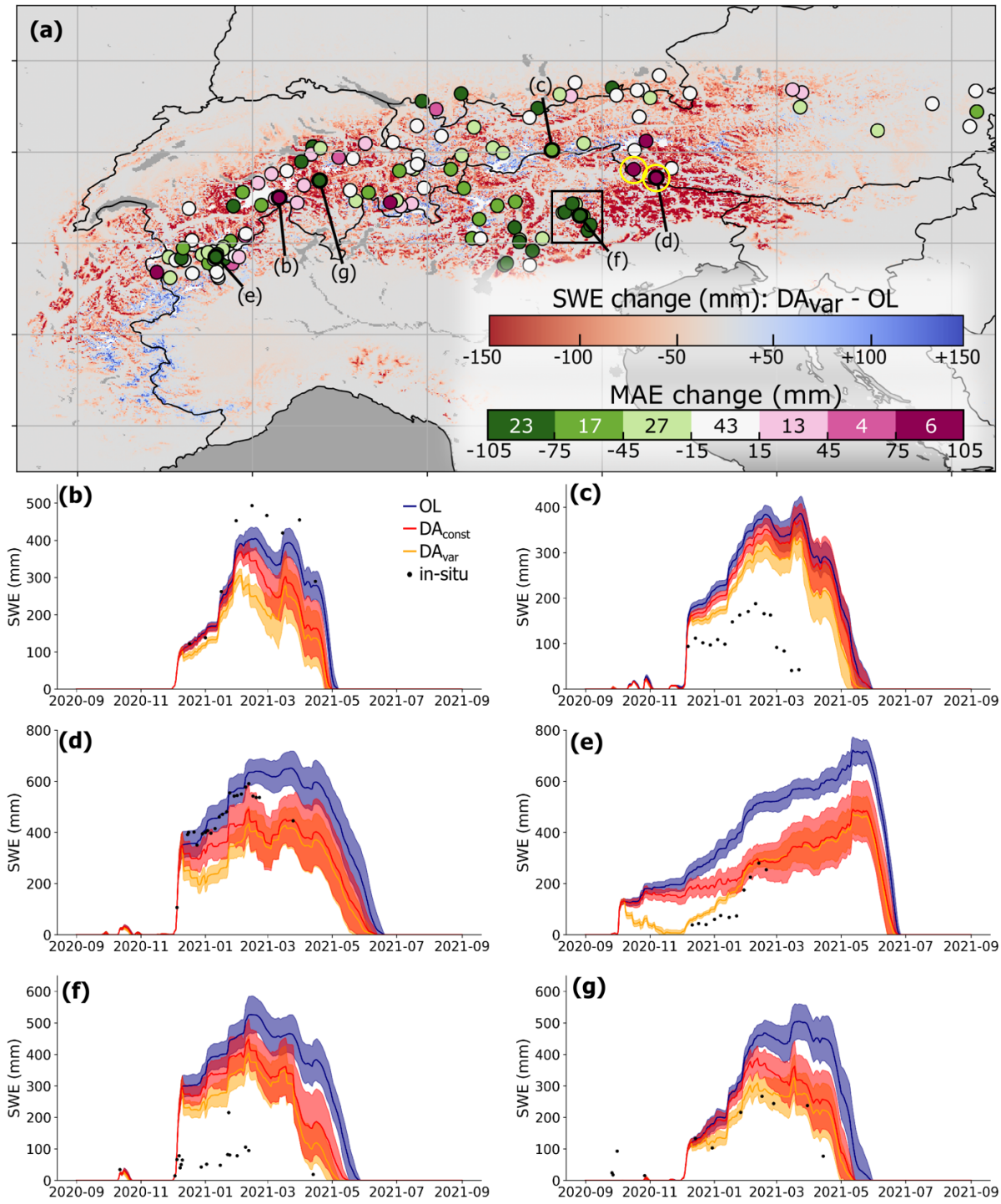

Figure S5 2021 SWE comparison. (a) Map of SWE changes (DA_{var} – OL), averaged during the period March 1 – 7, 2021. Sites with manual SWE measurements from the 2020/2021 snow season are plotted, colored according to the change in MAE between the DA_{var} and OL experiments. MAE changes are computed over the entire snow season. On the MAE change color bar, the number of sites that fall within each color range is indicated. (b-g) SWE timeseries from the three model experiments, compared with manual measurements (black dots) for in-situ measurement sites which are indicated in (a).

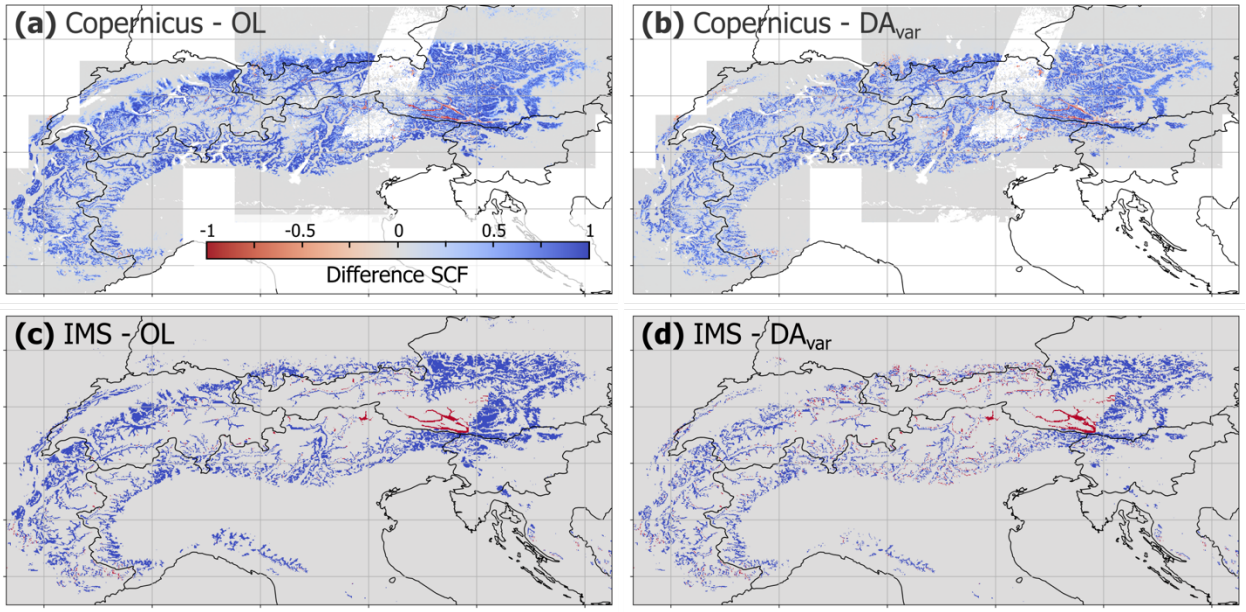

Figure S6 Comparison in modeled snow cover fraction (SCF) with two snow cover products on March 1, 2021. (a) SCF difference between Copernicus Fractional Snow Cover and OL experiment. White indicates data gaps. (b) SCF difference between Copernicus Fractional Snow Cover and DA_{var} experiment. (c) SC difference between IMS and OL experiment. (d) SC difference between IMS and DA_{var} experiment.

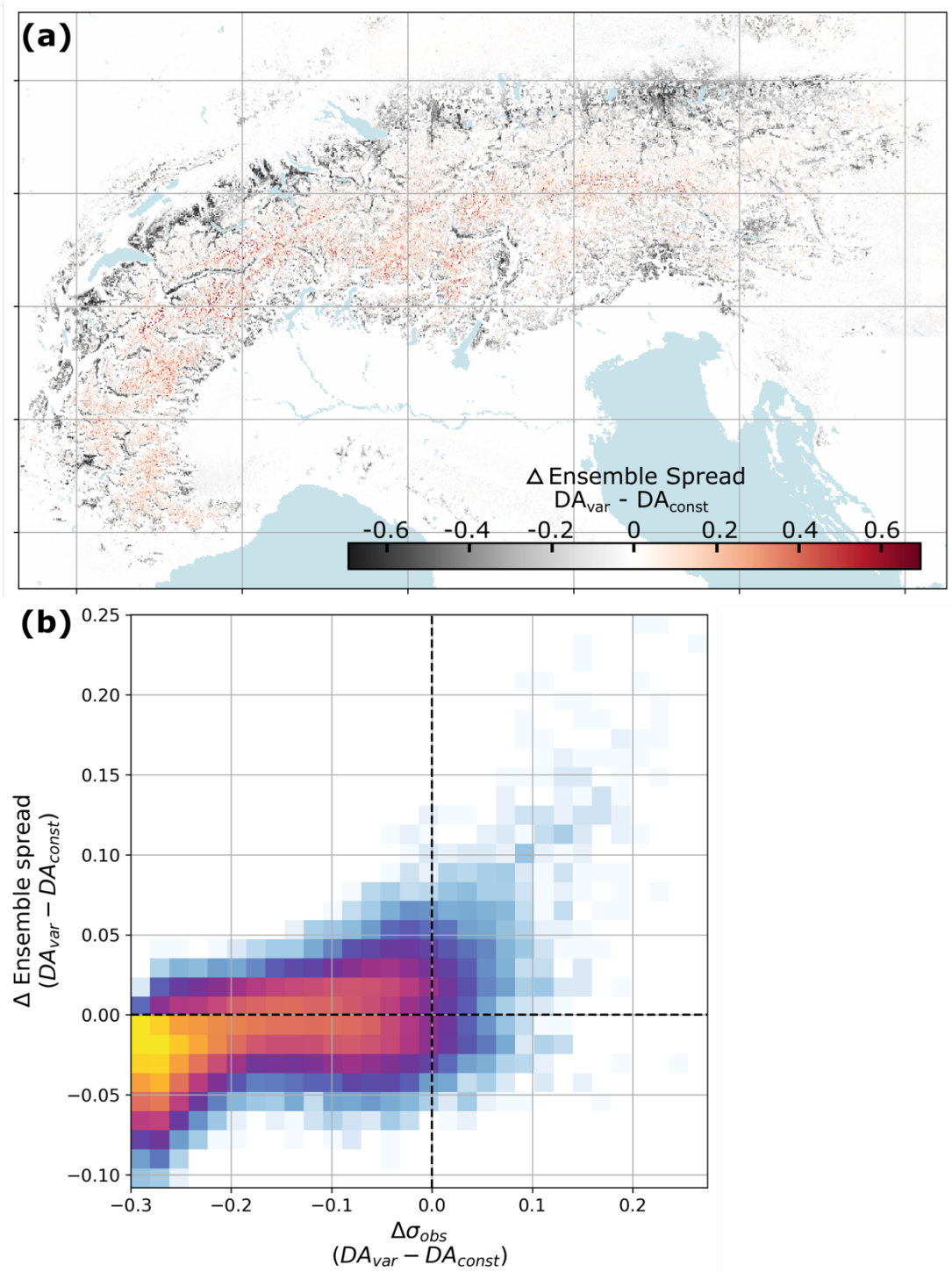

Figure S7 Impact of DA experiment on model ensemble spread. (a) Change in ensemble spread ($DA_{var} - DA_{const}$), averaged over the first week of March each year (March 1 - 7). (b) 2D histogram showing the change in ensemble spread with the change in observation uncertainty (σ_{obs}). Change in ensemble spread is taken over the first week of March (typically when SWE peaks) and change in observation uncertainty is taken over the full accumulation period leading up to the first week in March.

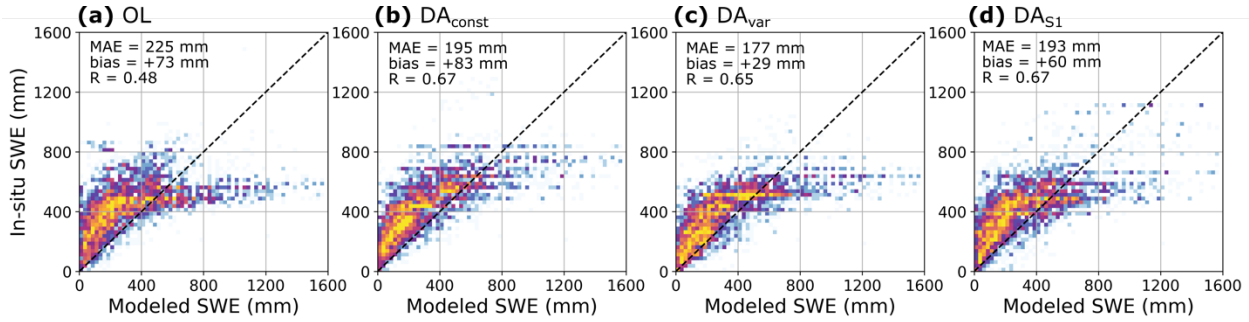

Figure S8 2D histograms comparing modeled SWE to in-situ SWE observations for (a) OL, (b) DA_{const}, (c) DA_{var}, and (d) DA_{S1}. The MAE, average bias, and R are provided for each approach.

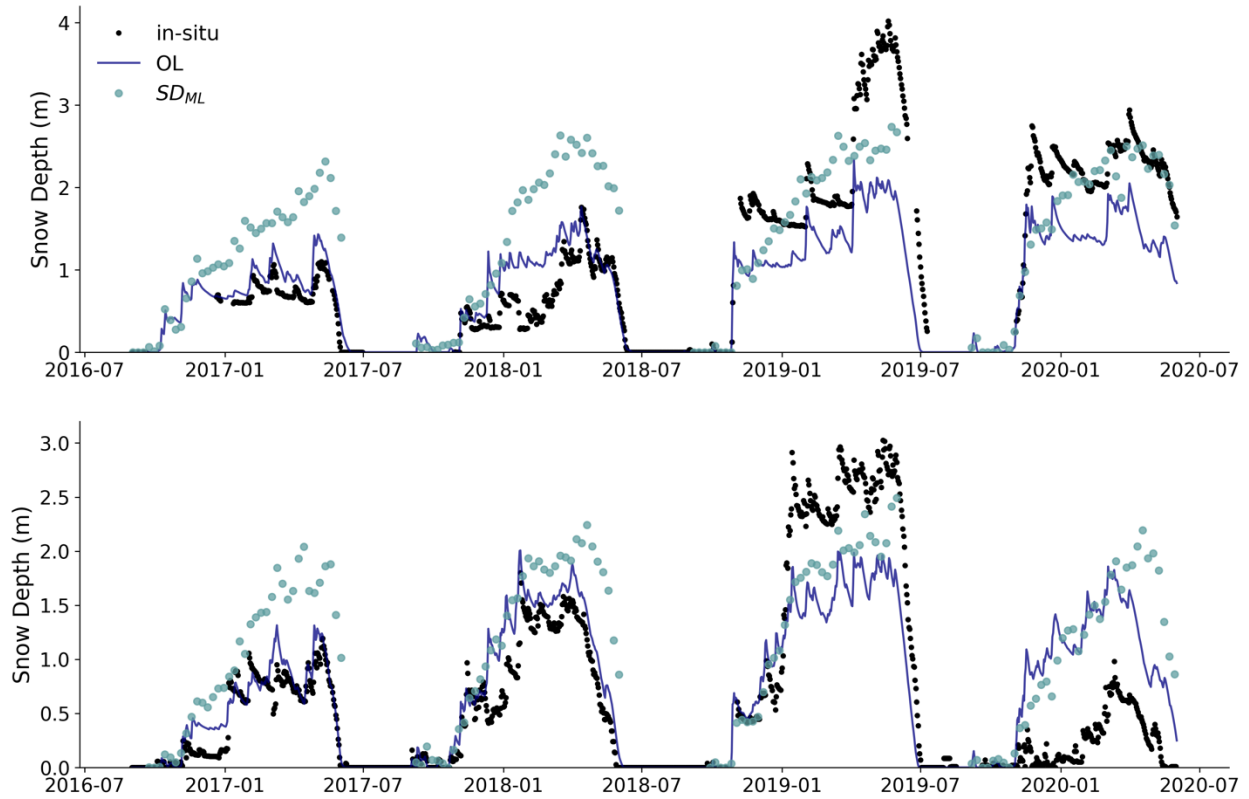

Figure S9 Snow depth timeseries at two example in-situ measurement locations, demonstrating interannual inconsistencies in model and assimilated observation (SD_{ML}) biases.